Tribology Transactions
Publication details, including instructions for authors and subscription information:
http://www.tandfonline.com/loi/utrb20

Influence of the Martensite Volume Fraction on the Reciprocating Sliding Behavior of Ti-Nb Microalloyed Steel

W. Tuckart [a] , D. Jenko [b] , N. Fochesatto [a] , F. Buezas [c] , H. Lorusso [d e] & H. Svoboda [e]

[a] Tribology Group, Engineering Department , Universidad Nacional del Sur CONICET-Bahía , Blanca , Argentina

[b] Institute of Metals and Technology , Ljubljana , SI-1000 , Slovenia

[c] Department of Physics , Universidad Nacional del Sur IFISUR-CONICET , Bahía Blanca 8000, Bs. As., Argentina

[d] Centro de Investigación y Desarrollo en Mecánica INTI , San Martín , Argentina

[e] Laboratorio de Materiales y Estructuras INTECIN , Facultad de Ingeniería UBA-CONICET , Buenos Aires , Argentina

Accepted author version posted online: 06 Nov 2013.Published online: 06 Nov 2013.

To cite this article: W. Tuckart , D. Jenko , N. Fochesatto , F. Buezas , H. Lorusso & H. Svoboda (2014) Influence of the Martensite Volume Fraction on the Reciprocating Sliding Behavior of Ti-Nb Microalloyed Steel, Tribology Transactions, 57:1, 146-155, DOI: 10.1080/10402004.2013.856981

To link to this article: http://dx.doi.org/10.1080/10402004.2013.856981

Tribology Transactions, 57: 146-155, 2014

ISSN: 1040-2004 print / 1547-397X online
DOI: 10.1080/10402004.2013.856981

STLE
Society of Tribologists and Lubrication Engineers

Influence of the Martensite Volume Fraction on the Reciprocating Sliding Behavior of Ti-Nb Microalloyed Steel

W. TUCKART,[1] D. JENKO,[2] N. FOCHESATTO,[1] F. BUEZAS,[3] H. LORUSSO,[4,5] and H. SVOBODA[5]
[1]Tribology Group, Engineering Department
Universidad Nacional del Sur
CONICET-Bahía Blanca, Argentina
[2]Institute of Metals and Technology
Ljubljana SI-1000, Slovenia
[3]Department of Physics
Universidad Nacional del Sur
IFISUR-CONICET, Bahía Blanca 8000, Bs. As., Argentina
[4]Centro de Investigación y Desarrollo en Mecánica
INTI, San Martín, Argentina
[5]Laboratorio de Materiales y Estructuras
INTECIN, Facultad de Ingeniería
UBA-CONICET, Buenos Aires, Argentina

The objective of this work was to evaluate the influence of martensite fraction on the wear mode and the energy dissipation by friction of dual phase (DP) steel tested under reciprocating sliding conditions. For this purpose, a Ti-Nb microalloyed steel was heat treated in a conventional furnace at temperatures between 780 and 880° C (intercritical annealing temperature) for 3 min to obtain DP microstructures with volume fractions of martensite between 25 and 90%. Wear tests were carried out in both DP and as-received samples, using a reciprocating tribometer with ball-on-flat geometry, at two constant applied loads, 2.5 and 4 N. The wear damage of each sample was measured through volume loss and the dissipated energy during the test. The obtained results evidenced a significant influence of the contact load over the wear mode, because at low load the DP wear was reduced with increased hardness but just up to 75% of martensite. At high load, the sliding process promotes an oxide mixture in the ferritic microstructure that acts as a factor in wear reduction.

KEY WORDS

Dual-Phase Steel; Sliding Reciprocating; Martensite

INTRODUCTION

High-strength low-alloy steels are a family of materials with interesting properties for many engineering applications. Dual-phase (DP) steels are part of this family and they essentially present a microstructure containing a ferritic matrix and colonies of martensite that can be promoted by intercritical annealing; that is, heat treatments at temperatures between Ac_1 and Ac_3. This is widely used to produce a dual-phase microstructure that can achieve ultimate tensile stress between 600 and 1,000 MPa, but it also includes combinations of ductility and a high strain hardening coefficient (Rashid *(1)*; Davies *(2)*). DPS are widely used by the automotive industry, and its applications have spread to parts subjected to wear, such as the transport of minerals and agricultural implements (Tyagi, et al. *(3)*).

According to Sawa and Rigney *(4)*, the wear behavior of DP steel depends strongly on the shape, size, and distribution of the martensite colonies. By using a grit paper abrasive against a steel wheel under high stress abrasion conditions, Modi, et al. *(5)* have shown that the wear rate is reduced with increasing martensite content of the material, but they detected a minimum wear rate when the martensite content was less than 47%. This is in agreement with Jha, et al. *(6)*, who found that a combination of ferrite and martensite offers better behavior under abrasive conditions, rather than coarse martensite.

On the other hand, several researchers (Wayne and Rice *(7)*; Abouei, et al. *(8)*, *(9)*; Saghafian and Kheirandish *(10)*) used sliding wear condition tests and concluded that regardless of the level of the applied load, the wear performance can be improved by increasing microstructural hardness due to the increase in the martensite fraction.

It is interesting to note that martensite's hardness is related to the carbon content in the austenite, which depends on the austenitization temperature and should also be related to the material's carbon content. Aksoy, et al. *(11)* have found a significant influence of the austenization temperature due to heat treatment. During this procedure, the carbon content in the

Manuscript received June 5, 2013
Manuscript accepted October 10, 2013
Review led by Richard Neu

austenite phase decreases when the austenitization temperature changes from critical temperature A_{C1} to A_{C3}. Then, the martensite volume proportion increases, but its hardness decreases, which leads to lower wear resistance.

Many wear studies have been performed on DP steels in the range of 0.2 wt% C and have been analyzed under several conditions. The influence of the martensite fraction over the wear rate is not completely clear, mainly because its contribution to the tribological performance depends strongly on the heat treatment parameters and the operating wear mechanism (Tyagi, et al. *(3)*; Sawa and Rigney *(4)*; Modi, et al. *(5)*; Jha, et al. *(6)*; Wayne and Rice *(7)*; Abouei, et al. *(8)*, *(9)*; Saghafian and Kheirandish *(10)*; Aksoy, et al. *(11)*).

In the present investigation, DP steel was obtained from a ferrous alloy with 0.088% carbon content, and attention has been focused on identifying the influence of the martensite fraction on the dry reciprocating wear behavior of DP steels obtained from Ti-Nb microalloyed steel. In order to discuss the wear mechanisms that developed during the tribological process, the relationship between wear volume and dissipated energy by friction for ball-on-flat bidirectional sliding contacts were correlated with those obtained from the bulk microhardness and wear mechanism and debris characterization.

In this study, it has been demonstrated experimentally that, for sliding reciprocating conditions, at low loads, the dual-phase wear volume was reduced inversely with the initial microstructure hardness but only up to 75% of martensite. When a high load was applied, the ferritic microstructure promoted a stable mixture of oxides that let the running-in overcome faster, and with lower wear damage, than the ferritic and martensitic material.

EXPERIMENTAL PROCEDURE

Materials and Methods

For this work, a sheet (made by Brasmetal Waelholzt, Brazil) with a chemical composition (wt%) of 0.088% C, 0.91% Mn, 0.314% Si, 0.024% P, 0.0072% S, 0.025% Nb, 0.075% Ti, 0.051% Al and the balance Fe was used.

The critical temperature transformation A_{C1} and A_{C3} were evaluated by dilatometry analysis, applying a heating and cooling rate of 15°C/min. Those temperatures were 768 and 890°C, respectively.

From the as-received material, consisting of a ferrite phase (BM), different volume fractions of martensite in the ferrite microstructures were obtained through intercritical annealing. These heat treatments were made heated at 15°C/min in a conventional furnace to temperatures of 780, 845, 860, and 880°C for 3 min followed by cold water quenching. Then, the volume fraction of martensite of 25% (DP25), 45% (DP45), 75% (DP75), and 90% (DP90) were quantified by quantitative metallography according to ASTM E562–08.

The microhardness was evaluated by Vickers at 10 N load on metallurgically prepared cross sections (Fig. 1). Due to the rolling process made by the metal producer, the base material shows a texture. BM samples were cut in normal and longitudinal cross sections with respect to the rolling direction. Thus, when the slide of the tribological test is made in the rolling direction, it is called longitudinal or BMl. In contrast, when the slide is applied in a perpendicular direction, it is called transversal or BMt.

In order to reveal the microstructure, the surface samples were at first ground manually using up to 2,000 grit abrasive paper and then polished with 0.5 μm of Al_2O_3 water-based slurries. Nital 2 reagent (100 mL ethanol and 2 mL nitric acid) was used for optical microscopy.

Sliding Wear Test

The wear tests were performed by means of a homemade reciprocating electrodynamic actuator tribometer according to ASTM G133 with a ball-on-flat geometry contact configuration.

The tests were performed at a frequency of 1.5 Hz with 10-mm oscillation amplitude for 50,000 continuous cycles. A standard WC ball (50% W/50% C) with a diameter of 5 mm was used as counterpart material and it was pressed onto the flat specimen, either BM or DP, with constant normal applied loads of 2.5 and 4 N. These normal forces were applied by means of a dead weight.

The initial maximun contact stress, p_0, was calculated in accordance with Eq. [1] from Hertz theory (Johnson *(12)*).

$$p_0 = \left[\frac{6P\,(E^*)^2}{\pi^3 R^2}\right]^{1/3}, \qquad [1]$$

where

$$\frac{1}{E^*} = \frac{1-\nu_1^2}{E_1} + \frac{1-\nu_2^2}{E_2}, \qquad [2]$$

where P is the applied load (N), R is the radius of the ball (mm), and E_{1-2} and υ_{1-2} are the Young's modulus and Poisson's ratios of the flat surface and ball, respectively. In Eq. [2] the following values were used for the steel: $\upsilon = 0.3$ and $E = 200$ GPa, and for the WC the following values were used (Shackleford, et al. *(13)*): $E = 680$ GPa and $\upsilon = 0.24$.

Maximum Hertzian contact pressures of 2,600 and 3,040 MPa were obtained at normal loads of 2.5 and 4 N normal loads, respectively.

The environment in the contact region was controlled by a thermostatic temperature chamber at 25 ± 2 °C and 35–45% relative humidity.

Prior to the test, the courterpart ball was cleaned in acetone in an ultrasonic bath and the flat surfaces were mechanically ground and polished with SiC 600 grinding paper (with a grain size around 26 μm) and then cleaned with ethanol.

The roughness (R_a) on the polished surface of the specimens ($0.06 \pm 1{\cdot}10^{-4}$ μm in the transverse direction and $0.11 \pm 2{\cdot}10^{-4}$ μm in the direction of sliding) was evaluated by means of profilometer measurements by using a Hommel Etamic T500 roughness meter.

After each test, the wear level was quantified through the volume of material loss, according to ASTM G133-05, and the width of the wear scar was examined by optical microscopy (OM) in order to determine the final maximum contact stresses. Assuming that the contact remains circular, this stress is calculated by dividing the applied load by the size of the final area. The reported wear results are the average values of between three and six tests, and the error bars (Fig. 2) show the standard error.

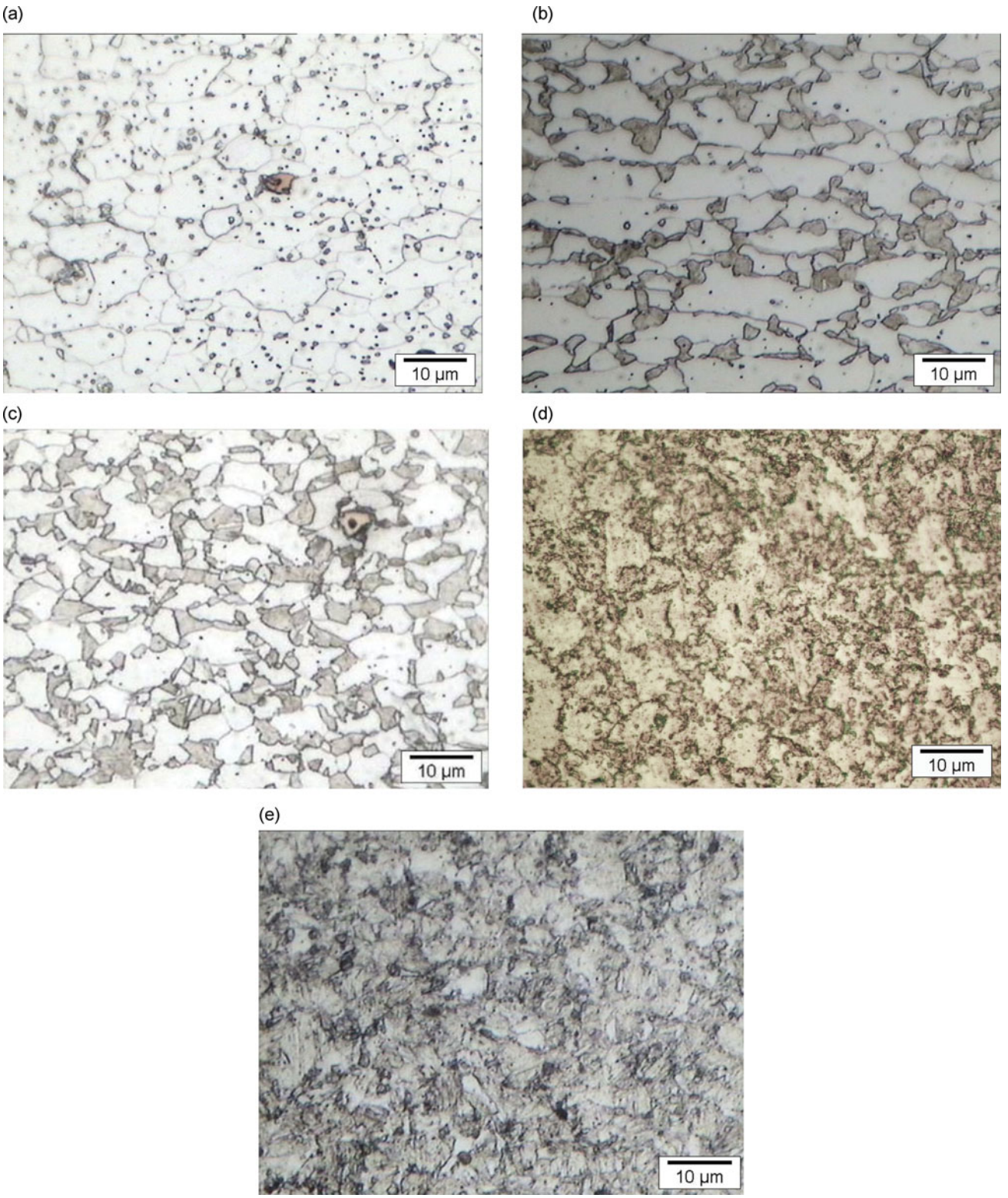

Fig. 1—Top-down OM image of microstructures at 1,000×: (a) BM, (b) DP25, (c) DP45, (d) DP75, and (e) DP90 (color figure available online).

The tribosurface was analyzed by OM and scanning electronic microscopy (SEM) with a secondary electrons detector. The tribo-oxides on the worn surface were also microanalyzed by energy-dispersive spectroscopy (EDS). After the test, the debris was collected and saved between two micro-slide glasses in order to understand the wear mechanism that developed during the sliding process.The debris was further investigated via high-resolution transmission electron microscopy and an analytical

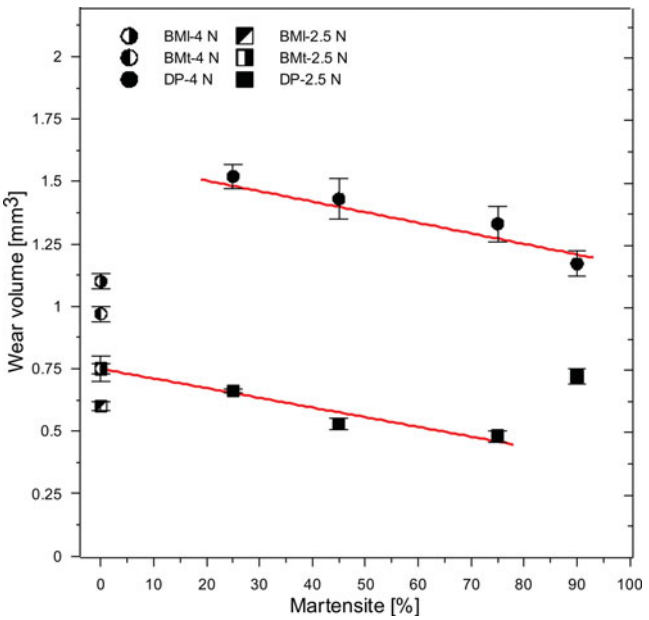

Fig. 2—Graphic of wear volume as a function of percentage of martensite for both samples (color figure available online).

EDS technique using a JEOL JEM-2100 at 200 kV accelerating voltage.

Debris specimens were applied on a 200-mesh Cu grid covered by a polymer thin film and coated with a carbon foil to prevent charging.

Estimate of Dissipated Energy by Friction

The mechanical energy of frictional contact is transformed and can be stored in the tribosystem or dissipated mainly through three processes: temperature increase, generation of new surfaces, and the entropy changes associated with material transformation at the interface (Ramalho and Miranda *(14)*).

According to Huq and Celis *(15)*, the wear volume of materials can be related to the dissipated energy, and the wear slope versus the dissipated energy curve is useful not only to contrast the wear resistance of different materials but to compare their wear resistance in various environmental conditions.

Although there are different approaches for bidirectional sliding ball-on-flat contact conditions, Huq and Celis *(15)–(17)* used the concept of cumulative dissipated energy, E_d, in order to demostrate that the wear of materials can be associated with the dissipation of frictional energy in sliding contacts, expressed as Eq. [3]:

$$E_d = \mu P v_s t, \qquad [3]$$

where t (s) is the duration of the sliding test, μ is the coefficient of friction, P is the applied normal load (N), and v_s is the relative sliding velocity (m/s).

This approach expresses that the energy that is dissipated in the contact can be calculated as the work of the friction force but taking into account the timescale over which the energy is released to the contacting materials.

By numerical simulation, Fouvry, et al. *(18)* concluded that most of the energy is assumed to be consumed by thermal dissipation and through third-body transformations.

In this article, for each test the energy dissipated by friction was estimated with the average value of the friction force calculated from the acquired friction force data. The friction force was also registered and fed into a computer via an interface (Vernier Labquest) as a function of time (1,250 data were saved).

RESULTS

Microstructural Characterization

Figure 1 shows the microstructural features of steel in different conditions (Table 1). The BM micrograph (Fig. 1a) shows a matrix of ferrite (dark) plus a precipitate of globular iron carbide (dark points) localized into the grains. The size of the ferrite grain was measured according to ASTM E112–96 as 7.2 ± 1 μm. The DP steels (Figs. 1b–1e) delineate a network of ferrite (light) plus martensite (dark). The volume fractions of martensite in DP25, DP45, DP75, and DP90 steels were 25 ± 5%, 45 ± 3%, 75 ± 5%, and 90 ± 2%, respectively. Table 1 represents the microhardness of all samples. It can be observed that the increase in the volume fraction of martensite has caused an increase in the hardness of DP steels.

As expected, the hardness results show that the ferrite microstructure has lower hardness than the DP material (Table 1). The increase in the volume fraction of martensite has also caused an increase in the hardness of DP microstructure.

Apart from the obtained microhardness results, a variation in the values between BM transversal and longitudinal samples is revealed. It is observed that when the martensite volume increased from 75 to 90%, the microhardness values rose significantly up to ~40%.

Wear Behavior

The obtained results of wear volume and microhardness as a function of martensite fraction are shown in Fig. 2. Additionally, the mean contact stresses measured after the test from the wear scar caused by the wear processes are shown in Table 2. From this, the BM (ferritic microstructure) presented a similar load-bearing capacity under both loads applied during the test.

There is also a variation in the wear behavior of the BM samples, with the relative orientation between the slide and the

TABLE 1—OVERVIEW OF MARTENSITE FRACTION AND VICKERS MICROHARDNESS VALUES OBTAINED FROM THE MICROSTRUCTURES TESTED

Sample	Intercritical Annealing Temperature (°C)	Martensite (%)	MicroVickers HV_1
BMt	—	—	188 ± 7
BMl	—	—	209 ± 7
DP25	780	25 ± 5	221 ± 10
DP45	845	45 ± 3	239 ± 5
DP75	862	75 ± 5	260 ± 1
DP90	880	90 ± 2	366 ± 30

TABLE 2—MEAN CONTACT STRESSES MEASURED FROM THE WEAR SCAR AFTER THE TEST

		Sample					
		BMl	BMt	DP25	DP45	DP75	DP90
Test Cycles	Applied Load (N)	Mean Contact Stress (MPa)					
50,000	2.5	16.7	21.1	19.0	23.9	22.7	17.5
	4.0	18.2	20.7	13.2	14.0	15.0	17.2
500			1,100	291	—	—	—

sheet-rolled directions. In the rolled direction lower wear is revealed, coinciding with an increase in hardness.

Analysis of the images of the worn surface showed different wear mechanisms. In the BM samples, an influence of microhardness can be inferred. The main wear mechanism developed was mild oxidative wear (Figs. 3a and 3b).

Although all of the martensite microstructures showed oxidative wear after the test, (Fig. 4a), the typical morphology of de-

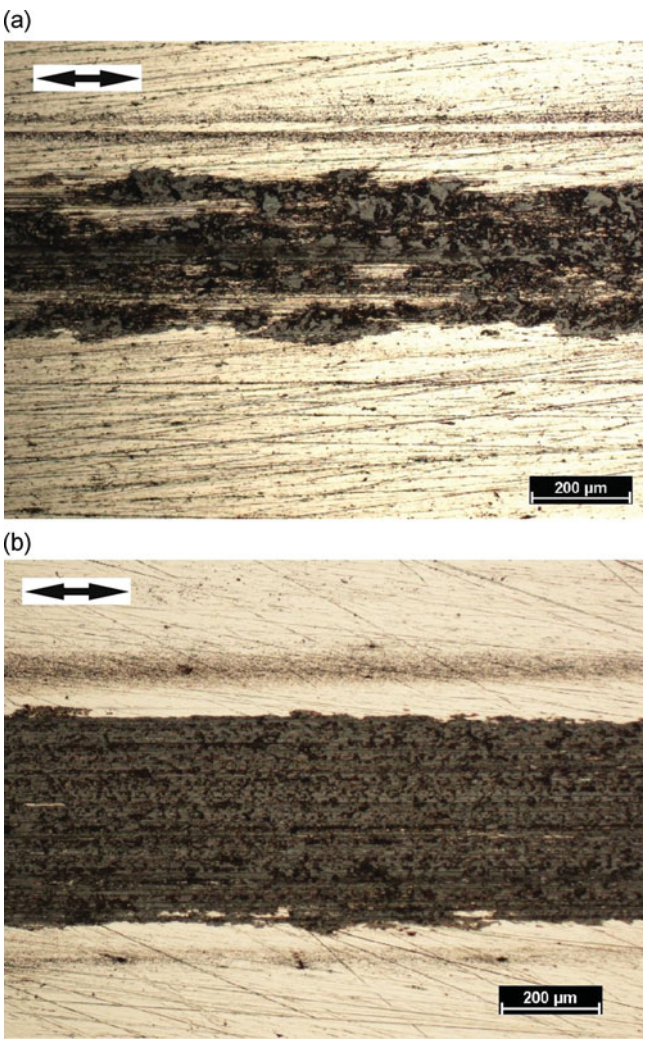

Fig. 3—Top-down OM image at 100× of worn surfaces after the test at 2.5 N load: (a) BMl and (b) BMt (color figure available online).

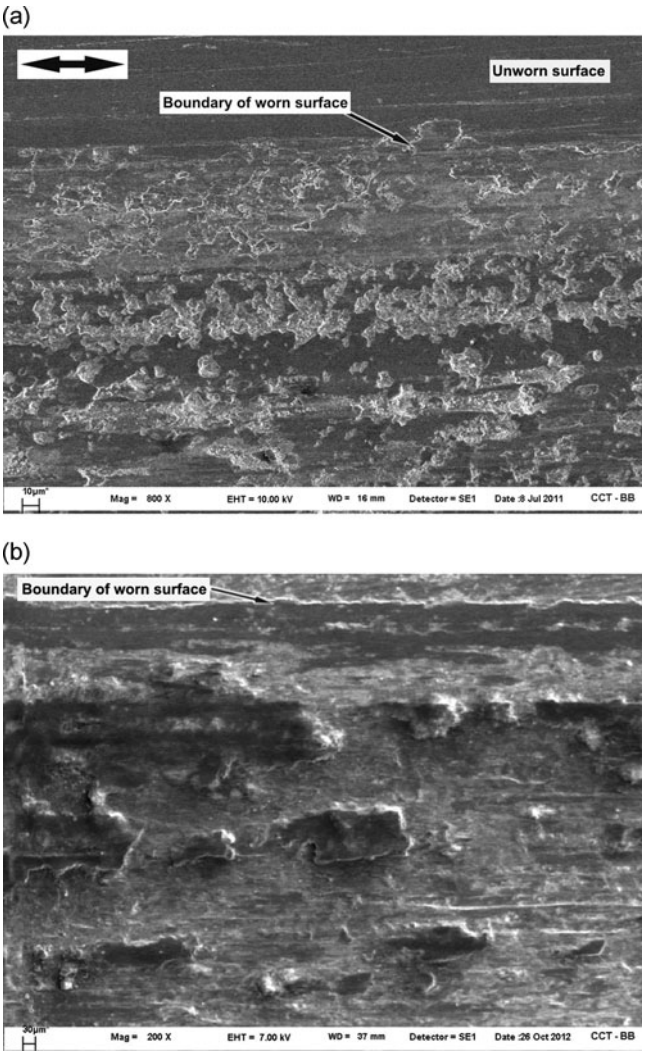

Fig. 4—Top-down SEM images of wear scar after the test at 2.5 N load: (a) DP25 at 800× and (b) DP90 at 200×.

lamination were was observed on the worn surface of the DP90 sample. This mechanism is evidenced in Fig. 4b. A mixture of iron oxides and several laminar metal particles collected from the DP90-2.5N samples can also be observed in Fig. 5.

On the other hand, there was no evidence of delamination on the wear scars of the DP45 and DP75 samples.

In comparison with the DP steel samples, a lower volume loss was measured for the BM samples when a load of 4.0 N was applied (Fig. 2). Several well-compacted smooth plateaus generated by oxidative wear were observed on the wear scar surface (Fig. 6a).

However, in the martensite specimens a reduction of the wear volume with an increase of the martensite fraction was observed. The best behavior on the DP samples was achieved for the DP90 specimen. After the test, oxidative damage and incipient laminar particles appearing by delamination were detected as the main wear mechanism (Fig. 6b). These mechanisms can be confirmed from the debris shown in Fig. 7, where reddish brown tribo-oxides collected after the test from the DP75–4N sample and particles

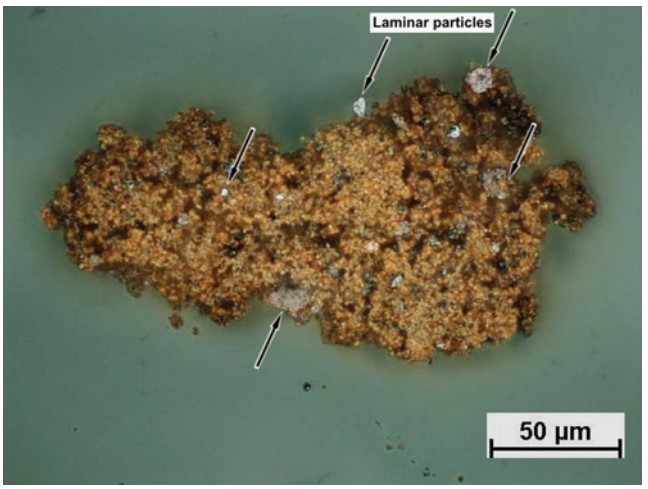

Fig. 5—OM image at 500×: debris of DP90 sample tested at 2.5 N. Brown and black tribo-oxides and laminar particles can be observed (color figure available online).

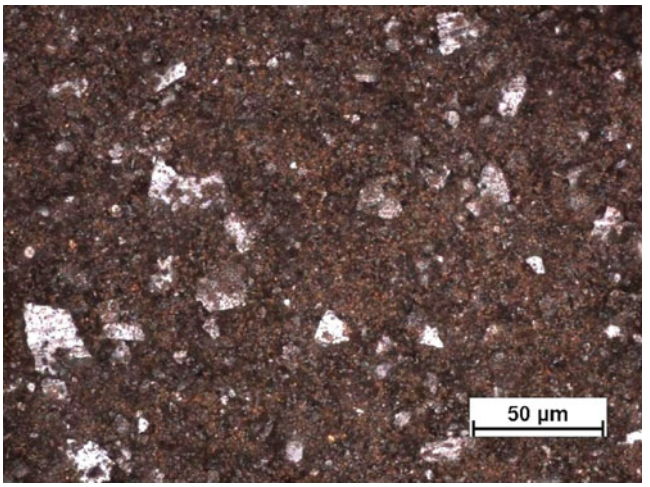

Fig. 7—OM image at 500× of debris of DP75 specimen tested at 4 N load. Brown tribo-oxides and laminar particles can be noticed (color figure available online).

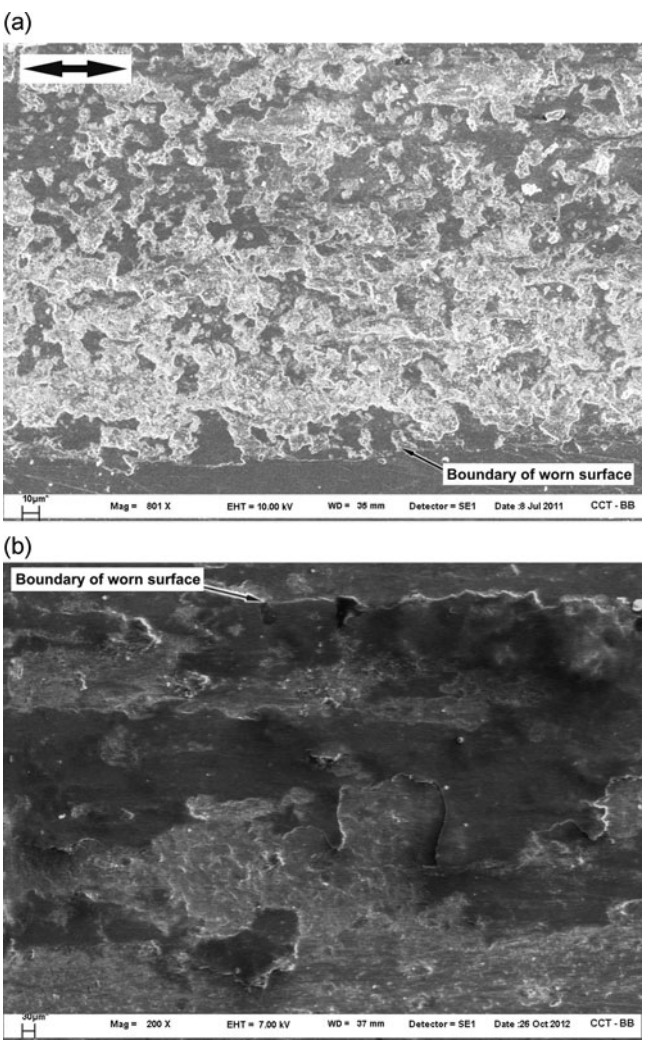

Fig. 6—Top-down SEM images of wear scar after the test at 4 N load: (a) BMt at 800× and (b) DP75 at 200×.

with metal laminar fragments can be observed. Similar fragments were found in other DP samples.

Additionally, in the wear scar of the DP25 sample, scratches due to abrasive wear were observed. Its morphology on the boundary region of the wear scar is shown in Fig. 8.

The atomic percentage results obtained with EDS-TEM of the collected debris show that for BM-4N samples only iron and oxygen were detected with different atomic percentage ratios (O%/Fe% = 0.7, 1.0, and 0.3). This fact suggests that during the friction process, ferrous oxides like FeO and a mixture of other iron oxides were formed.

On the other hand, the analysis of debris from DP25–4N showed the presence of oxygen, iron, and tungsten (Figs. 9a and 9b) with approximate ratios (at%) of 0.25 O/0.5 Fe/0.25 W. Because these values do not match any known FeWO phase, we can

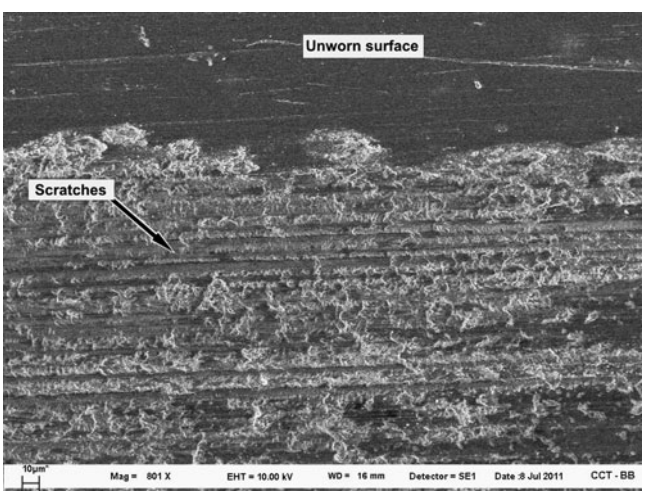

Fig. 8—Top-down SEM image at 800× of the wear scar of the DP25 specimen after the test at 4 N load.

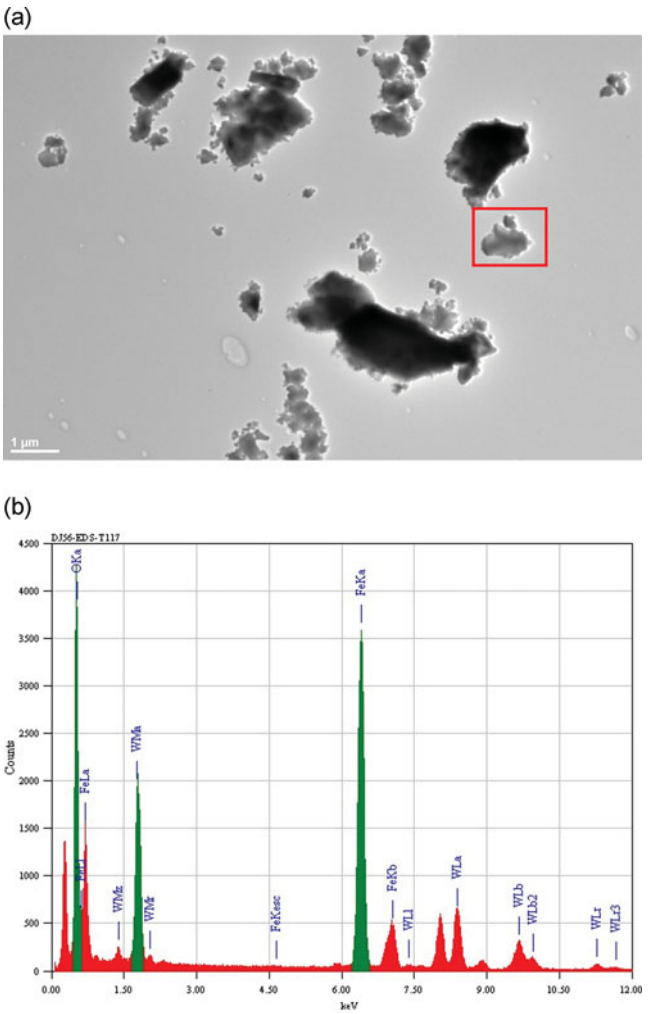

Fig. 9—TEM image at 2,000×: (a) EDS and (b) debris from the DP25 sample tested at 4 N load. Peaks of iron, oxygen, and tungsten can be observed (color figure available online).

also infer the development of oxide mixtures (International Centre for Diffraction Data *(19)*).

Energy Dissipated by Friction

The results presented in Fig. 10 show the relationship between the volume loss and the total energy dissipated by friction. A linear tendency can be inferred including the BMt and BMl at 2.5 and 4 N loads and the dual-phase material tested at low load. Moreover, another linear approximation that crosses the first one is evidenced from DP90 tested at 2.5 N (indicated with an arrow) and the dual-phase: DP45, 75, and 90. Finally, an upper point on the right side of the plot corresponds to sample DP25 tested at 4 N load, which shows the highest dissipated energy and has no correlation with other points in the plot.

On the basis of the remarkable difference in wear behavior between BMt and DP25 samples tested at 4 N load, we decided to focus on the study of the running-in process of these samples and the analysis of its influence on wear process. Thus, after 500 cycles and applying Eq. [3], the energy dissipated by friction was 3.12 and 4.50 J for BMt and DP25, respectively.

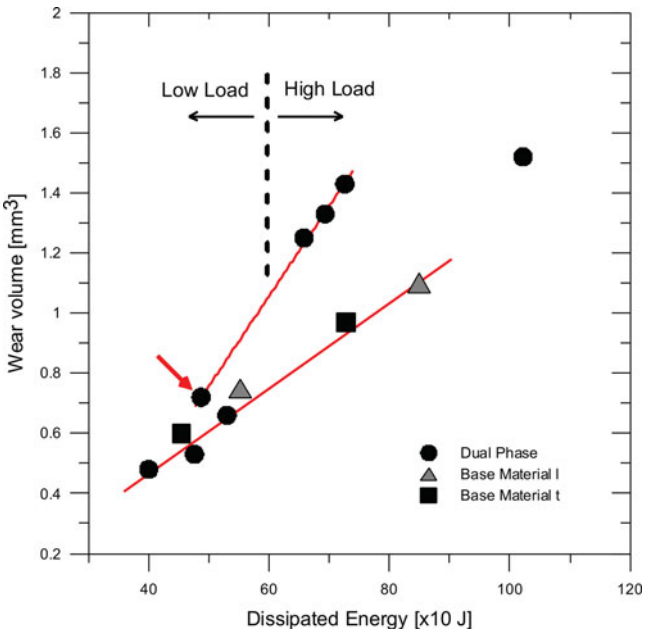

Fig. 10—Wear volume as a function of energy dissipated by friction during each test. The arrow shows the point of the DP90–2.5 N sample (color figure available online).

A micrograph of the worn surface of the BM sample (Fig. 11a) depicts the development of a well-compacted oxide layer of ~80 mm width. The SEM-EDS analysis in several spots of the wear track showed a ratio (at%) of 2:1 O/Fe; that is, the wear scar evidences a mixture of iron oxides.

On the other hand, the micrograph of the DP25 specimen (Fig. 11b) exhibits a wider scar (150 μm) with severe damage by sliding wear and some highly fragmented iron oxides. The quantitative EDS analysis of differents zones showed only a ratio (at%) of 1:1 O/Fe, which evidences the presence of an FeO phase.

DISCUSSION

Low Load Test

When a load of 2.5 N was applied, the wear process is mainly restricted to oxidative wear (Fig. 2), and abrasion with debris ejection from the contact zone was also observed. Thus, the wear rate initially decreased with an increase in martensite content up to 75%.

Moreover, when the material with the highest martensite volume fraction (90%) was evaluated, the wear increased again. In this condition, though tribosurfaces with oxidative damage were observed after several thousand stress cycles near the tribosurface, the wear process was controlled by a fatigue wear mechanism (Fig. 4b). This phenomenon was corroborated with the laminar debris that can be observed in Fig. 5.

In the same sense, a comparison between wear and microhardness results seems to have no direct correlation (Fig. 2 and Table 1). Increasing the microhardness (from 188 to 260 HV) initially leads to a lower wear volume, due to the resistance

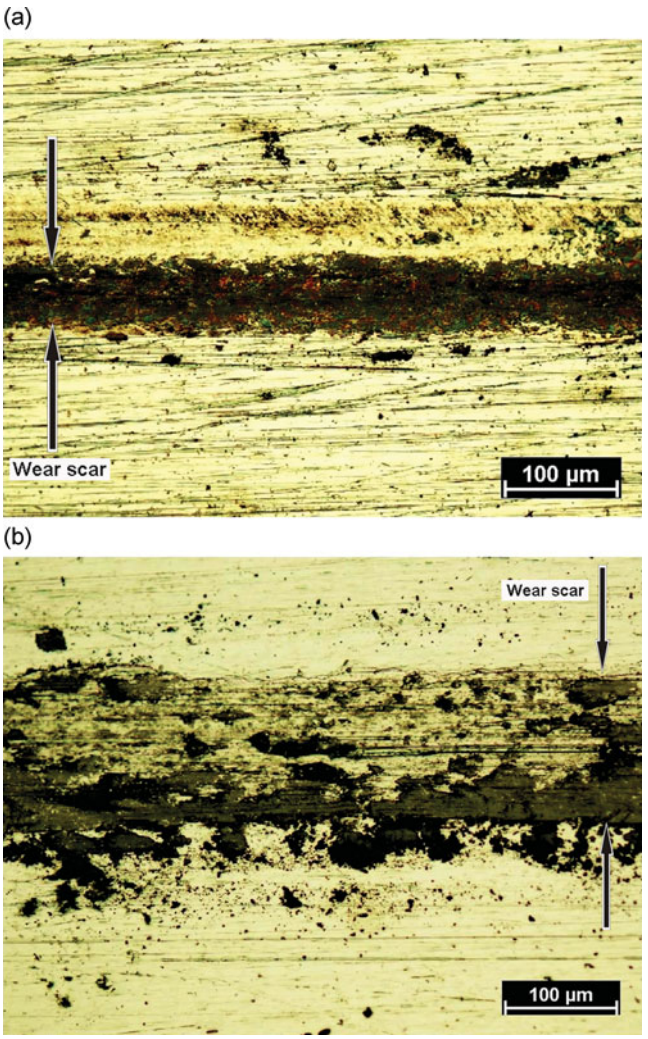

Fig. 11—Top-down OM image at 200× of the worn surface for samples tested at 4 N load after 500 cycles: (a) BMt sample and (b) DP25 (color figure available online).

offered by the specimen surface. However, at a higher hardness level (360 HV), the wear damage increases again, due to brittle fragmentation of material, which is related to the high amount of martensite phase.

This performance is similar to the results found by Modi, et al. *(5)*, who studied high abrasion tests of DP with 0.2 wt% carbon. No improvement in wear resistance was observed when the martensite content increased beyond 39.2% (206 HV) due to the fact that the abrasive particles (40 μm) were comparable to the size of the major fraction of martensite colonies. In addition, in tests made with similar steel alloys and test conditions, Jha, et al. *(6)* found that both a microstructure with low hardness (155 HV) and another one with a fully martensitic microstructure (451 HV) showed an inferior wear response than one with a combination of ferrite and martensite.

Figure 10 shows two linear relationships between wear volume and cumulative dissipated energy. According to Huq and Celis *(17)*, the wear rate can be represented by the slope of volumetric wear as a function of the dissipated energy plot. Therefore, the linear correlation implies that the same wear mechanism is operative (Huq and Celis *(16)*). Thus, a good agreement can be inferred from the relationships observed in Fig. 10 and the wear mechanisms after the tribological process, which are shown in Figs. 2–8.

Though the point related to DP 90-2.5N (indicated with an arrow in Fig. 10) does not show a higher level of dissipated energy, it seems to be in direct correlation with the points that correspond to the DP material tested at 4 N. This condition can be attributed to the additional development of delamination wear (Figs. 4b and 5).

High Load Test

When the test load increased to 4 N, the comparative analysis of wear volumes on the martensite fraction shows a different performance than that at 2.5 N, because the wear process is being controlled by other wear mechanisms.

In addition, under this load condition the hardness seems to have no direct correlation with the wear volume (Fig. 2), because increasing the hardness from 188 HV (ferritic microstructure) to 221 HV (ferrite plus 25% martensite) initially leads to a higher loss of wear volume. With a further increase in microhardness, the wear rate decreases due to the resistance of the martensite phase (Table 1) to abrasive damage. Thus, when a high load was applied, the best behavior was found with BM, but the performance of DP samples is in agreement with the results reported by Saghafian, et al. [9] from tests made with similar volume fractions of dual phase. Instead, they had used a POD with a flat end—that is, a conformal geometry—and carried the tests out with a contact stress that was several times lower than those employed in the present work.

Because the WC has a high hardness (~2,800 HV) and its Young's modulus is three times higher than that of steel, transfer will be prevented and hardening and agglomeration of the debris will be produced on the steel surface. Thus, with DP microstructures, after a short sliding distance, the FeO oxide layer gets removed, increasing surface damage. This type of oxide has intrinsically lower adherence to metal substrates than other iron oxides (Sakrani and Sullivan *(20)*), and this explains the better behavior of BM-4N compared to DP25-4N during the running-in stage (Figs. 12a and 12b).

The obtained results let us infer that when a load of 4 N was applied, during the running-in the debris generation from a pliant ferritic microstructure promotes third-body layer formation. This layer consists of a stable mixture of oxides debris accumulation and is able to protect rubbing between the metal and WC counterpart. This is in accordance with the energy dissipated by friction and the load-bearing capacity after 500 cycles measured between BM and DP25 (Table 2).

Furthermore, in the relationship between wear volume and the dissipated energy plot (Fig. 10) for DP45, 75, and 90% of martensite, a linear increase in the wear volume at increasing cumulative friction energy can be noticed; that is, the same wear mechanisms were operating (oxidative plus delamination wear). BMt and BMl, by oxidative wear, show the same linear fit with samples tested at low load.

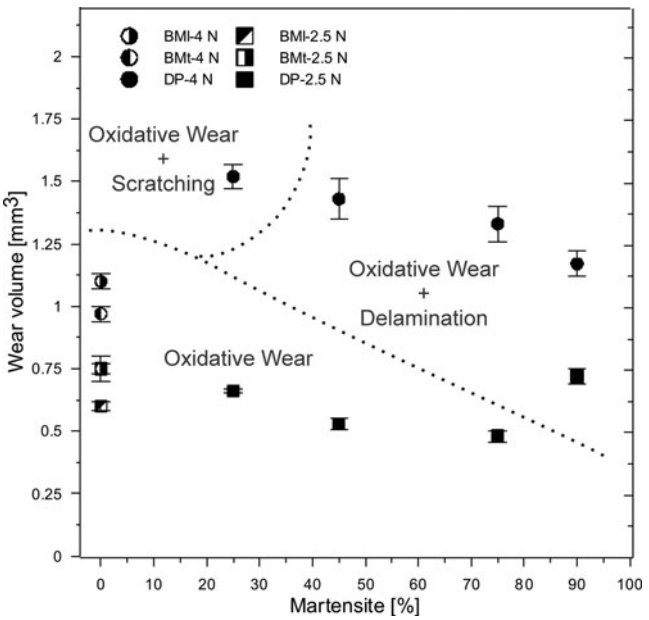

Fig. 12—Plot overview with the map of the hypothesized wear mechanisms that developed during the tests.

DP25 samples exhibited the highest wear volume in the present study (Fig. 2), which could be caused by the development of a combination of oxidative and abrasion wear.

From the EDS TEM spectrum analysis it was observed that the DP25 sample debris contained W, which could proceed from the WC counterpart. As mentioned above, WC has a hardness of ~2,800 HV and the iron oxides have a hardness of 600–700 HV (Godfrey *(21)*). We postulate that the hardness of iron oxide debris is not enough to promote debris generation by abrasion of the WC counterface observed in Fig. 9a.

However, taking into account both the presence of FeO on the wear track, which is formed above 530°C, and the higher dissipated energy, which is higher than in the other DP samples (Fig. 10), it is possible to infer that there is tungsten oxidation (it is known that this process begins above 500–600°C; Pierson *(22)*). Therefore, the iron debris was oxidized after its generation, whereas tungsten debris could oxidize in the contact spots. Thus, mixing and accumulation of W and Fe oxides was facilitated (Figs. 9a and 9b). When this mixture cools down, it creates other highly abrasive particles in addition to iron oxides. This heightens the abrasion component in the tribosystem, which is consistent with the scratches due to abrasion wear damage observed in Fig. 8.

The influence of the abrasion component on the global wear volume of the tribosystem decreases on DP samples, when microstructural hardness increases. The wear results and surface images (Figs. 2, 6–8) suggest that, due to the protection of the hard (martensite) phase, the influence of the abrasion stage is more significant on the wear volume than the delamination wear mechanism.

An overview plot of the wear mechanisms observed during the wear sliding test is shown in Fig. 12.

CONCLUSIONS

On the basis of the results obtained from the study of the influence of martensite fraction volume on the dry reciprocating behavior of Nb-Ti microalloy steel against WC, the following conclusions can be drawn:

- Regardless of the applied load, in this kind of contact the tribological behavior depends on the microstructure features and the content of ferrite and martensite phases, but no direct correlation between its hardness and the volume loss was found.
- The wear was compared with the accumulated friction work dissipated through the interface. The relationships between both of them gave a linear fit when the same dominating wear mechanisms were operating.
- The predominant wear mechanisms can be classified into three categories. For a low wear level oxidative wear was the main wear mechanism, whereas for medium volume loss, oxidative wear and fatigue contact were both predominant. Finally, the higher wear volume level was measured when the mechanism of wear by oxidation and abrasion became dominant.

ACKNOWLEDGEMENTS

The authors express their appreciation for the support given to the Engineering Department of Universidad Nacional del Sur and especially we wish to thank Ing. German Prieto-UNS and Dr. Marcelo Failla from PLAPIQUI-UNS for their valuable discussions.

REFERENCES

(1) Rashid, M. (1979), "Formable HSLA and Dual Phase Steels," *Proceedings of the TMS-AIME Conference "Relationship between Microstructure and Formability in Formable HSLA and Dual Phase Steels*," A.T. Davenport, ed., TMS-AIME, Warrendale, PA.

(2) Davies, R. G. (1978), "Influence of Martensite Composition and Content on the Properties of Dual-Phase Steels," *Metallurgical Transactions*, **9A**, pp 671–676.

(3) Tyagi, K., Sath, S., and Ray, S. (2004), "Development of Wear Resistant Medium Carbon Dual Phase Steels and Their Mechanical Properties," *Materials Science and Technology*, **20**, pp 615–652.

(4) Sawa, M. and Rigney, D. A. (1987), "Sliding Behavior of Dual-Phase Steels in Vacuum and Air," *Wear*, **119**, pp 369–390.

(5) Modi, O., Prasad, B., and Jha, X. (2003), "Low Stress Wear Be-C Steel: Influence of Microstructure and Test Parameters," *Tribology Letters*, **15**, pp 249–235.

(6) Jha, X., Prasad, B., and Modi, O. (2003), "Correlating Microstructural Features and Mechanical Properties with Abrasion Resistance on a High Strength Low Alloy Steel," *Wear*, **254**, pp 120–128.

(7) Wayne, S. and Rice, S. (1983), "The Role of Microstructure in Wear of Selected Steel," *Wear*, **85**, pp 93–106.

(8) Abouei, V., Saghafian, H., and Kheirandish, Sh. (2007), "Effect of Microstructure on the Oxidative Wear Behavior of Plain Carbon Steel," *Wear*, **262**, pp 1225–1231.

(9) Abouei, V., Saghafian, H., Kheirandisha, Sh., and Ranjbar, Kh. (2008), "An Investigation of the Wear Behaviour of 0.2% C Dual Phase Steels," *Journal of Materials Processing Technology*, **203**, pp 107–112.

(10) Saghafian, H. and Kheirandish, Sh. (2007), "Correlating Microstructural Features with Wear Resistance of Dual Phase Steel," *Materials Letters*, **61**, pp 3059–3063.

(11) Aksoy, M., Karamq, M. B., and Evin, E. (1996), "An Evaluation of the Wear Behaviour of a Dual-Phase Low-Carbon Steel," *Wear*, **193**, pp 248–252.

(12) Johnson, K. L. (1985), *Contact Mechanics*, Cambridge University Press: Cambridge, UK.

(13) Shackleford, J. F., Alexander, W., and Park, J. S. (1994), *CRC Materials Science and Engineering Handbook*, CRC Press: Boca Raton, FL.

(14) Ramalho, A. and Miranda, J. C. (2006), "The Relationship between Wear and Dissipated Energy in Sliding Systems," *Wear*, **260**, pp 361–367.

(15) Huq, M. Z. and Celis, J. P. (2002), "Expressing Wear Rate in Sliding Contacts Based on Dissipated Energy," *Wear*, **252**, pp 375–383.

(16) Huq, M. Z. and Celis, J. P. (1997), "Reproducibility of Friction and Wear Results is Ball-on-Disc Unidirectional Sliding Tests of TiN-Alumina Pairings," *Wear*, **212**, pp 151–159.

(17) Huq, M. Z. and Celis, J. P. (1999), "Fretting Wear of Multilayered Ti,Al/NrTiN Coatings in Air of Different Relative Humidity," *Wear*, **225–229**, pp 53–64.

(18) Fouvry, S., Liskiewicz, T., Kapsa, Ph., Hannel, S., and Sauger, E. (2003), "An Energy Description of Wear Mechanisms and Its Applications to Oscillating Sliding Contacts," *Wear*, **255**, pp 287–298.

(19) International Centre for Diffraction Data. (1993), *Mineral Powder Diffraction File, Data Book*, International Centre for Diffraction Data: Swarthmore, PA.

(20) Sakrani, S. and Sullivan, J. (1998), "Iron Oxide Films in Tribological Surfaces of Alloy Steel," *Proceedings of the SPIE*, **3**, pp 175–179.

(21) Godfrey, D. (1999), "Iron Oxides and Rust (hydrated iron oxides) in Tribology," *Lubrication Engineering*, **55**, pp 33–37.

(22) Pierson, H. O. (1999), *Handbook of Chemical Vapor Deposition (CVD): Principles, Technology, and Applications*, 2nd ed., William Andrew: New York.